An Optimization-Based UWB-IMU Fusion Framework for UGV

Shuaikang Zheng, Zhitian Li, Yunfei Liu, Haifeng Zhang, and Xudong Zou, *Member, IEEE*

***Abstract*—UWB and IMU fusion positioning methods have been widely concerned for its high accuracy and robustness in GNSS-denied environment. However, most of the existing methods are stay under the Markov assumption and ignore the credible estimation of the yaw angle. In this paper, we propose a novel tightly-coupled IMU and multiple UWB tags fusion framework based on a graph optimization model that is able to provide high precision positioning and attitude determination service, which provides a new technical approach for the practical application of UWB and IMU fusion. A relative rotation and motion state initialization algorithm is designed and presented, which solves the problems that IMU installation direction is difficult to measure and the initial state is not stationary in practical application. Simulation experiments shows the impact of UWB tags distribution distance and IMU noise parameters on system performance, which provides design reference for practical applications. Finally, the real-site experiment proves the positioning RMSE of 4 cm based on our fusion solution and these simulation evidences, which confirms the great performance of our fusion solution.**

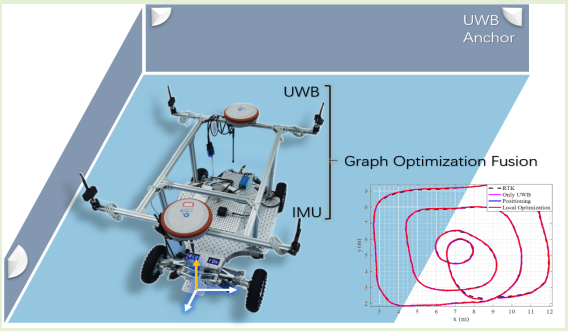

***Index Terms*—UWB, IMU, fusion positioning, graph optimization.**

I. Introduction

IN RECENT years, UGVs (Unmanned Ground Vehicle) have been increasingly used in military, civilian and commercial fields, such as logistics, surveillance, search, rescue, mining, plant protection, etc. [1]. For the positioning of UGV in indoor environment, related research has been conducted for decades [2]. Among the positioning technologies, UWB (Ultra-Wideband) has been widely concerned with the advantages of high time resolution, anti-multipath, low power consumption, high ranging accuracy, and high security [3], [4]. Another classic and most commonly used positioning technology – inertial navigation has the advantages of fast response speed and no environmental impact, so that it can provide short-term accurate information about the device's motion, which means it can be used to compensate for the high positioning error caused by UWB ranging jitter, and to improve positioning accuracy and robustness. Therefore, the fusion of UWB and inertial navigation has naturally become one of the hot issues in the field of UWB positioning [5]–[9].

The general UWB/IMU (Inertial Measurement Units, the sensors for inertial navigation) fusion methods are largely dependent on the Bayesian filtering framework [10]–[13] like EKF (Extended Kalman Filter). However, the basic idea of these filter-based methods is stay under the Markov assumption [14]. That is, they assume that current state is correlated only with the previous state and the current observation, which leads to the underuse of information.

To address this problem, optimization-based sensor fusion and state estimation are gradually favored [15]. The graph optimization approach originated from the vision-based SLAM (Simultaneous Localization and Mapping) [16], [17] are in the ascendant, and achieve excellent result compared with traditional filter-based methods. By using this technique, we will present a localization framework based on graph optimization,

Manuscript received September 2, 2021; revised January 10, 2022; accepted January 16, 2022. Date of publication January 19, 2022; date of current version February 28, 2022. This work was supported in part by the National Key Research and Development Program of China under Grant 2018YFB2002300; in part by the Key Research Program of Frontier Science, CAS, under Grant ZDBS-LY-JSC028; and in part by the Beijing Municipal Natural Science Foundation under Grant 4202080. The associate editor coordinating the review of this article and approving it for publication was Dr. Qammer H. Abbasi. *(Corresponding authors: Zhitian Li; Xudong Zou.)*

Shuaikang Zheng, Yunfei Liu, and Haifeng Zhang are with the State Key Laboratory of Transducer Technology, Aerospace Information Research Institute, Chinese Academy of Sciences, Beijing 100190, China, and also with the School of Electrical and Communication Engineering, University of Chinese Academy of Sciences, Beijing 100049, China (e-mail: zhengshuaikang18@mails.ucas.ac.cn; liuyunfei17@mails.ucas.ac.cn; zhanghaifeng19@mails.ucas.ac.cn).

Zhitian Li is with the State Key Laboratory of Transducer Technology, Aerospace Information Research Institute, Chinese Academy of Sciences, Beijing 100190, China (e-mail: ztli@mail.ie.ac.cn).

Xudong Zou is with the State Key Laboratory of Transducer Technology, Aerospace Information Research Institute, Chinese Academy of Sciences, Beijing 100190, China, also with the School of Electrical and Communication Engineering, University of Chinese Academy of Sciences, Beijing 100049, China, and also with the Qilu Aerospace Information Research Institute, Chinese Academy of Sciences, Jinan 250100, China (e-mail: zouxd@aircas.ac.cn).

Digital Object Identifier 10.1109/JSEN.2022.3144660

which can easily fuse different kinds of measurements and obtain high-precision positioning results with a sliding trajectory window.

In addition, how to obtain high-precision attitude information is still a challenge for range-based positioning system. Although attitude can be estimated by integrating the gyroscope measurement [18], [19], it also undergoes a drift over time. Geomagnetic measurement based method is the other common technic route which use the measured geomagnetic north as a reference for attitude estimate [20], [21], but the indoor magnetic disturbances are so severe that it is intolerable for many robot applications. Visual inertial odometer (VIO) aided method is a newly emerging route to obtain pose with 6 degrees of freedom [22], [23]. However, this route requires high computing power and a suitable environment. Our solution is to mount multiple UWB modules on the robot, and use the geometric relationship between them to obtain a credible single-shot measurement of yaw angle.

The proposed UWB and IMU fusion model jointly imposes the range and pre-integration constraints over a sliding window that has several characteristics: (i) It supports single-shot estimation of position and attitude at the same time. (ii) It estimates the position and attitude more accurately with a sliding state window; (ii) It adopt a reference frame window optimization strategy to ensure real-time operation in some low power systems; (iv) It is robust to outliers due to fusion with an outlier rejection algorithm. The main contributions of this paper are summarized as:

- A tightly-coupled fusion method of multi-UWBs and IMU based on graph optimization model is proposed. Compared with the traditional UWB/IMU combined positioning scheme, this method not only greatly improves the positioning accuracy, but also supports accurate heading estimation, which further expands its application possibilities.
- An optimization method of relative rotation between equipment and system initial state in motion is presented, which achieves effective and stable results in related experiments, and solves the problems of IMU installation direction not easy to measure and dynamic initialization in practical application.
- In a large number of simulation and real-site experiment, the influence of different UWB tags distribution distances and IMU noise parameters on system performance are analyzed, which provides a system design reference and promotes the process of practical application. Real-site experiment results with a positioning RMSE of 4cm proves the great performance of the proposed fusion framework.

The rest of this paper is structured as follows. In Section II, we introduce the composition of our system. Preprocessing for both UWB ranging and IMU pre-integration are presented in Section III. A tightly coupled, nonlinear optimization-based UWB/IMU fusion procedure is presented in Section IV. Experimental results are shown in Section V. Finally, this paper is concluded with the discussion and possible future research directions in Section VI.

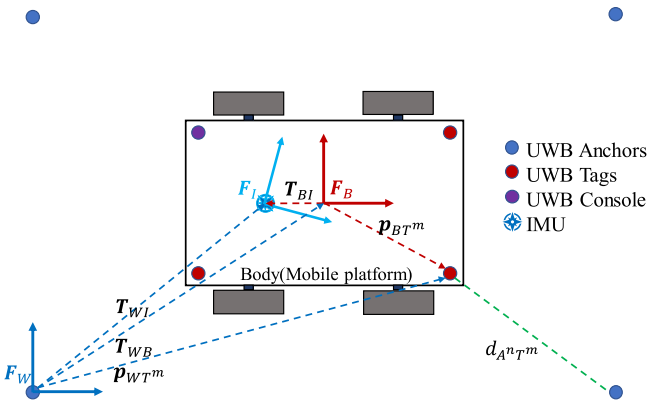

Fig. 1. System composition diagram. Our system includes 4 UWB anchors, 3 UWB tags, 1 UWB console, and 1 6-DOF IMU. A ranging measurement is generated between each UWB tag and UWB anchor. IMU provides acceleration and angular velocity measurement.

II. System Deployment

The system composition is shown in Fig. 1. The main goal of this system is to get the position and attitude of the mobile platform (Body) by fusing UWB and IMU. Firstly, 4 UWB anchors are arranged in the operating space of the Body, then 3 UWB tags and an IMU are installed on the Body. UWB anchors communicate with each tag through TW-TOF (Two Way Time of Flight) for ranging. The ranging between anchor n and tag m is expressed as $d_{A^nT^m}$. In addition, a UWB console is used in the system, which is only responsible for collecting all ranging measurements and sending them to the host computer. It takes 20ms to complete a round of UWB ranging, and the data sampling frequency of IMU is 200Hz. For convenience, N and M represent the total number of UWB anchors and tags, and n and m respectively represent one of them.

The system involves a variety of devices and sensors, and there are different reference frames and related coordinate conversion. The reference frame is expressed as F, such as F_W on UWB anchors, F_B on Body and F_I on IMU. The rotation and translation transformations in three-dimensional space are expressed as $\mathbf{T} = [\mathbf{R}|\mathbf{p}]$, where $\mathbf{R} \in \mathrm{SO}(3)$ represents rotation and $\mathbf{p} = \begin{bmatrix} p^x & p^y & p^z \end{bmatrix}^T \in \mathbb{R}^3$ represents translation. $\mathbf{v} = \begin{bmatrix} v^x & v^y & v^z \end{bmatrix}^T$ represents velocity. The transformation F_B relative to F_W is expressed as $\mathbf{T}_{WB} = [\mathbf{R}_{WB}|\mathbf{p}_{WB}]$, similar to $\mathbf{T}_{WI} = [\mathbf{R}_{WI}|\mathbf{p}_{WI}]$ and $\mathbf{T}_{BI} = [\mathbf{R}_{BI}|\mathbf{p}_{BI}]$.

Therefore, the position of UWB anchor n in F_W is expressed as $\mathbf{p}_{WA^n}$. The relationship between the UWB tag position $\mathbf{p}_{WT^m}$ and the body pose $[\mathbf{R}_{WB}|\mathbf{p}_{WB}]$ relative to F_W is:

$$\mathbf{p}_{WT^m} = \mathbf{p}_{WB} + \mathbf{R}_{WB}\mathbf{p}_{BT^m} \tag{1}$$

where $\mathbf{p}_{BT^m}$ is the prior position of UWB tag m in F_B. This formula also reflects the geometric relationship between different UWB tags, which is convenient for the construction of the optimizer.

III. Optimization Model and Measurement Constraint

Our system uses a graph optimization model (Fig. 2) to fuse sensor data and estimate Body state. In graph optimiza-

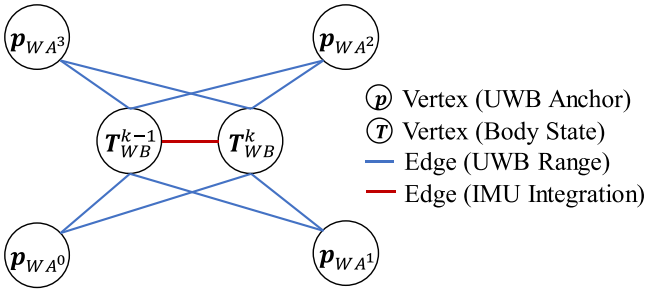

Fig. 2. System graph optimization model. In our optimization model, $\mathbf{p}_{WA}$ is used as a fixed vertex and $\mathbf{T}_{WB}$ (include $\mathbf{v}_{WB}$) at different time are used as the vertexes to be optimized; The UWB range and IMU pre-integration are used as edges to provide measurement constraints.

tion model, we only need to set the vertices representing the variable state and the edges representing the constraint conditions. The graph optimization library we use is G2O (General Graph Optimization) [24]. Here we focus on the correlation measurement and residual construction used in our model. According to the characteristics of UWB range and plane motion of UGV, we propose UWB ranging constraint and plane motion constraint. Moreover, we use pre-integration in [25] as IMU pre-integration constraint.

A. UWB Ranging Constraint

In the traditional method, the position of each UWB tag can be obtained by trilateral positioning separately, and then solve the attitude by geometric relationship between them. However, this method is not conducive to the improvement of the overall accuracy, because it is easy to be affected by individual measurements and the error of each tag position will be accumulated to attitude. Therefore, we propose a method based on the graph optimization model to directly use all ranging measurements to solve the Body position and attitude. This method can make full use of all UWB ranging data, avoid the influence of single extreme ranging, and is easy to fuse with other data.

Assuming UWB range error conforms to Gaussian distribution $\mathcal{N}(0,\sigma)$, based on (1) we can know the UWB range observation model is:

$$d_{A^nT^m} = \|\mathbf{p}_{WA^n} - (\mathbf{p}_{WB} + \mathbf{R}_{WB}\mathbf{p}_{BT^m})\|_2 + \mathcal{N}(0,\sigma) \quad (2)$$

where $\mathbf{p}_{WA^n}$ indicates the position of UWB anchor n, $\mathbf{p}_{BT^m}$ indicates the position of UWB tag m in F_B, $d_{A^nT^m}$ indicates the ranging between anchor n and tag m. Therefore, for anchor n and tag m, the error function in our optimization model is expressed as follows:

$$e_{A^nT^m} = \|\mathbf{p}_{WA^n} - (\mathbf{p}_{WB} + \mathbf{R}_{WB}\mathbf{p}_{BT^m})\|_2 - d_{A^nT^m} \quad (3)$$

The error functions determined by all range are combined into column vectors:

$$\mathbf{e}_{AT} = \begin{bmatrix} e_{A^1T^1} & \cdots & e_{A^1T^M} & \cdots & e_{A^NT^M} \end{bmatrix}^T \quad (4)$$

The total error term of UWB is:

$$E_{uwb} = \rho(\mathbf{e}_{AT}^T \boldsymbol{\Sigma}_U \mathbf{e}_{AT}) \quad (5)$$

where ρ is Huber robust cost function, $\boldsymbol{\Sigma}_U$ is the information matrix of UWB ranging. We solve this optimization problem with Gauss-Newton algorithm implemented in G2O in order to get $\mathbf{p}_{WB}$ and $\mathbf{R}_{WB}$. Note that our system can obtain a single-shot estimation of pose, which can meet the stable pose measurement requirements of some scenes.

B. IMU Pre-Integration Constraint

For IMU, we use the IMU pre-integration constraint in our optimization model like [25]. The corresponding IMU error functions are:

$$\begin{aligned} \mathbf{e}_R &= \mathrm{Log}(\Delta\mathbf{R}_{ij}^{-1}\mathbf{R}_{IW}^i\mathbf{R}_{WI}^j) \\ \mathbf{e}_v &= \mathbf{R}_{IW}^i\left(\mathbf{v}_{WI}^j - \mathbf{v}_{WI}^i - \mathbf{g}\Delta t_{ij}\right) - \Delta\mathbf{v}_{ij} \\ \mathbf{e}_p &= \mathbf{R}_{IW}^i\left(\mathbf{p}_{WI}^j - \mathbf{p}_{WI}^i - \mathbf{v}_{WI}^i\Delta t_{ij} - \frac{1}{2}\mathbf{g}\Delta t_{ij}^2\right) - \Delta\mathbf{p}_{ij} \end{aligned} \quad (6)$$

The IMU total error term E_{imu} is:

$$E_{imu}(i,j) = \rho([\mathbf{e}_R^T\mathbf{e}_v^T\mathbf{e}_p^T]\boldsymbol{\Sigma}_I[\mathbf{e}_R^T\mathbf{e}_v^T\mathbf{e}_p^T]^T) \quad (7)$$

where ρ is Huber robust cost function, $\boldsymbol{\Sigma}_I$ is the information matrix of IMU pre-integration.

In addition, due to F_I and F_B is not aligned, the following transformation is needed in order to achieve the goal of Body pose optimization.

$$\begin{aligned} \mathbf{R}_{WI} &= \mathbf{R}_{WB}\mathbf{R}_{BI} \\ \mathbf{p}_{WI} &= \mathbf{p}_{WB} + \mathbf{R}_{WB}\mathbf{p}_{BI} \\ \mathbf{v}_{WI} &= \mathbf{v}_{WB} + \left[\boldsymbol{\omega}_{WB}\right]_\times \mathbf{R}_{WB}\mathbf{p}_{BI} \\ \boldsymbol{\omega}_{WB} &= \mathbf{R}_{BI}\boldsymbol{\omega}_B \end{aligned} \quad (8)$$

where $\left[\boldsymbol{\omega}_{WB}\right]_\times$ is the antisymmetric matrix of the instantaneous spin axis of $\mathbf{R}_{WB}$.

In this way, the IMU can be used to provide short-term motion constraints of the Body state.

C. Plane Motion Constraint

According to the plane motion characteristics of UGV, the corresponding plane constraint is designed in our optimization model. The plane height constraint assumes that the Body moves up and down very little and the plane attitude constraint assumes that only the yaw angle changes during the motion. The corresponding error function is:

$$\mathbf{e}_{plane} = \begin{bmatrix} \mathbf{p}_{WB}^z - z_{fixed} \\ \mathbf{R}_{WB}\cdot\begin{bmatrix}0 & 0 & 1\end{bmatrix}^T - \begin{bmatrix}0 & 0 & 1\end{bmatrix}^T \end{bmatrix} \quad (9)$$

where $\mathbf{p}_{WB}^z$ is z-axis coordinate of Body, z_{fixed} the is height of the Body running plane.

The total error term of the plane motion constraint is:

$$E_{plane} = \rho(\mathbf{e}_{plane}^T\boldsymbol{\Sigma}_{plane}\mathbf{e}_{plane}) \quad (10)$$

where ρ is Huber robust cost function, $\boldsymbol{\Sigma}_{plane}$ is the information matrix of plane motion. The error term ensures the stability of Body height and attitude in the optimization process, and avoids the influence of UWB or IMU data jitter. Note that this constraint is optional according to system characteristics, which means that it is not necessary for a pure

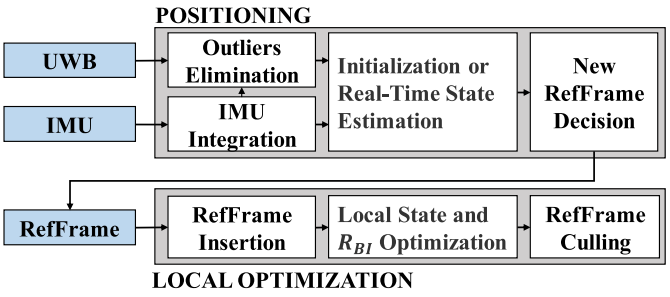

Fig. 3. System framework. The system includes two threads: real time positioning and local optimization.

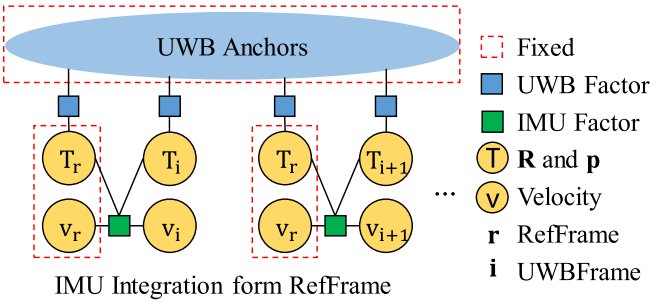

Fig. 4. Optimization model of real time positioning method. The Latest updated RefFrame state is used as the IMU constraint reference.

two-dimensional system. We use this constraint to preserve the ability of our system to adapt to three-dimensional motion.

So far, all error terms in the system optimization model have been constructed.

IV. Algorithm Framework

The system framework is shown in Fig. 3. The system consists of two threads, real-time positioning thread and local optimization thread. The positioning thread includes the preprocessing of UWB and IMU data, the initialization of Body state, and the real-time state estimation with UWB/IMU fusion. Local optimization is performed in a separate thread to avoid interfering with real-time operation. In this thread, local RefFrames are optimized together to get a higher precision state, which provides the constraint reference for the positioning thread.

The concepts of UWBFrame and RefFrame involved in the system are described as follows. UWB Data is the ranging between all UWB tags and anchors in a period (20ms), and IMU Data is the data of accelerometer and gyroscope sampled at a certain time. UWB-IMU Frame (referred to as UWBFrame) is the data composed of UWB Data and all IMU Data (aligned according to their timestamp) from the current time to the latest RefFrame (or next-to-last RefFrame). The RefFrame is the UWBFrame with fewer ranging outliers and certain time interval with other RefFrames (see Section IV-B).

A. Initialization

The initialization process is to provide the initial pose and velocity for the system, and determine the first RefFrame. If the initialization is performed in Body static state, we only use the UWB error term E_{uwb} (5) to solve the Body position and attitude, and sets the velocity to $\mathbf{0}$. Otherwise, in the motion state, we use the RefFrames in the local optimization thread for joint optimization to determine the velocity of the initial state (see Section IV-D). The related description of local optimization will be introduced in Section IV-C. In any case, we always select the earliest UWBFrame with less UWB ranging outliers as the first RefFrame, and the judgment is based on E_{uwb} calculated by the optimized state.

B. Real-Time Positioning

In the real-time positioning thread, we fuse IMU pre-integration and UWB ranging at the data level to directly get the position, attitude and velocity of Body (referred to as tightly coupling). The graph optimization model is shown in Fig. 4. The IMU pre-integration starts from the latest RefFrame or the next-to-last RefFrame to the current UWBFrame, which depends on whether the state of the latest RefFrame in the local optimization thread is updated. If it is updated, the latest RefFrame state is used as the IMU constraint reference, otherwise, the next-to-last RefFrame state is used. The state to be optimized is the pose and velocity of current UWBFrame j, and the set is $\theta^j = \mathbf{R}^j_{WB}, \mathbf{p}^j_{WB}, \mathbf{v}^j_{WB}$. The state of the RefFrame is fixed during optimization, and the IMU constraint can imply the effect of the plane constraint in a short change time, so the error term is the joint of E_{uwb} and E_{imu}, and the optimization function is:

$$\theta^j = \underset{\theta j}{\operatorname{argmin}} \left((E_{\text{uwb}}(j) + E_{imu}(i, j) \right) \tag{11}$$

The reason for using RefFrame instead of last UWBFrame state as the IMU constraint reference is that the state of RefFrame after local optimization is more accurate and stable, that is to say, it can provide more accurate IMU constraint. In this way, we can overcome the jitter of pure UWB positioning and the drift of pure IMU integration, and obtain more accurate real-time positioning results.

In addition, because of the possible outliers in UWB ranging measurements, we eliminate the large deviation value in them according to the optimization results of UWB/IMU fusion, to provide better measurements for local optimization thread. By applying the 3-σ rule, we consider one observation range to be an outlier if it meets:

$$\left| d_{A^n T^m} - \|\mathbf{p}_{WA^n} - (\mathbf{p}_{WB} + \mathbf{R}_{WB}\mathbf{p}_{BT^m})\|_2 \right|_{abs} > 3\sigma \tag{12}$$

where $\mathbf{p}_{WB}$ and $\mathbf{R}_{WB}$ are the optimization results of (11). If the number of range outliers in current UWBFrame is less than 5, this UWBFrame can be used as a candidate RefFrame. On this basis, if the time interval from previous RefFrame is large enough, which depends on the computing power, we select this UWBFrame as a RefFrame.

C. Local Optimization

As shown in Fig. 5, the local optimization thread forms the local window with the RefFrames continuously inserted by the real-time positioning thread. The state θ^W to be optimized are pose and velocity of all RefFrames in the local

TABLE I
NOISE PARAMETERS OF IMU

IMU	IMU0	IMU1	IMU2	IMU3	IMU4
Acc. N.D.	1.0e-0	1.0e-1	1.0e-2	1.0e-3	1.0e-4
Gyro. N.D.	1.0e-1	1.0e-2	1.0e-3	1.0e-4	1.0e-5
Acc. B.V.	1.0e-2	1.0e-3	1.0e-4	1.0e-5	1.0e-6
Gyro. B.V.	1.0e-3	1.0e-4	1.0e-5	1.0e-6	1.0e-7

Parameters of different IMU. Acc. N.D. (Accelerometer Noise Density, $m/s^2/\sqrt{Hz}$), Gyro. N.D. (Gyroscope Noise Density, $rad/s/\sqrt{Hz}$), Acc. B.V. (Accelerometer Bias Variations, $m/s^2\sqrt{Hz}$), Gyro. B.V. (Gyroscope Bias Variations, $rad/s\sqrt{Hz}$).

TABLE II
RELATIVE ROTATION OPTIMIZATION

Setting	0.00	5.00	10.00	20.00	30.00	45.00	90.00
Result	2.30	6.62	8.71	20.50	27.38	51.84	89.08
Error	2.30	1.62	1.29	0.50	2.62	6.83	0.92

Optimization results of different relative rotation. The data in the table are degree (°).

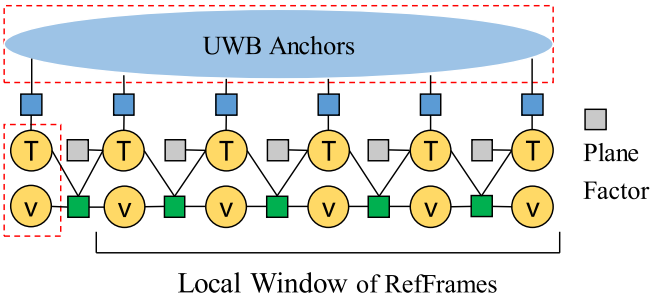

Fig. 5. Local optimization model. The state of the RefFrame before the optimization window is fixed, and the state of all the RefFrames in the window is to be optimized.

window. The constraints are all corresponding UWB range, IMU pre-integration between adjacent RefFrames, and plane motion constraint. The state of the RefFrame before local window is fixed, which only provides the IMU constraint reference. The total optimization function is:

$$\theta^W = \underset{\theta W}{\operatorname{argmin}}(\sum\nolimits_{i\in Window}(E_{\text{uwb}}(i) + E_{imu}(i-1,i) + E_{plane}(i))) \quad (13)$$

Local RefFrames optimization can make full use of reliable data with high SNR (Signal Noise Ratio), and provide reliable RefFrame state constraints for positioning thread, so as to improve the overall positioning accuracy. This also means that it is not necessary to optimize state of all UWBFrame, thereby saving computing time. After the optimization, the older frame in the window is moved out, and the next round of optimization is continued after a new RefFrame is inserted. Note that the local optimization thread is an independent thread. On this way, even if this thread cannot run in real time in some low power systems, it can ensure that the positioning thread runs in real time with high precision, which enhances the adaptability of our algorithm on different devices.

D. Optimization of Initial State and Relative Rotation

In practical application, the solution of relative translation between F_B and F_I requires complex motion of Body to overcome the problem of observability. Fortunately, it is easy to measure manually. However, the relative rotation is not easy to be measured directly. In view of this, we propose an initialization method of relative rotation. The optimization function is the same as (13), except that the $\mathbf{R}_{BI}$ is also regarded as a variable to be optimized when building the optimizer.

Before the local optimization, only UWB ranging is used for RefFrame selection and pose state initialization. After waiting for enough RefFrames to be inserted, the joint optimization of local window is carried out to get the relative rotation and the state of all RefFrame together. At the same time, the velocity initialization is completed, which solves the problem of initialization in motion state (undertake Section IV-A). After the initialization of state and relative rotation, the UWB/IMU tightly-coupled fusion in the real-time positioning thread can be carried out.

V. EXPERIMENT

A large number of simulation and real-site experiments are carried out to fully verify the reliability and effectiveness of our system, and explore the influence of various factors on the system performance. In these experiments, the RMSE of the proposed hierarchical algorithms is compared quantitatively. The comparison algorithms include: Only UWB, which only uses UWB ranging to optimize, as shown in (5); Positioning, UWB/IMU fusion in our real-time positioning thread, as shown in (11); Local Opt., optimization of RefFrames window (the window size is 20) in our local optimization thread, as shown in (13).

A. Simulation Experiment

Firstly, we carry out simulation experiments to verify the effectiveness of our framework, and analyze the influence of different UWB tags distribution distances and IMU noise parameters on the system performance, as well as the optimization ability for the relative rotation between F_B and F_I. In the simulation, 4 UWB anchors are set to form a square with a side length of 20 m, and 3 UWB tags form an equilateral

TABLE III
POSITIONING AND HEADING ERROR (m | °) OF 5 SEQUENCES

Sequence	Only UWB	Positioning	Local Opt.
Seq. 1	0.050 | 1.72	0.043 | 1.43	0.040 | 1.26
Seq. 2	0.049 | 1.78	0.042 | 1.43	0.039 | 1.20
Seq. 3	0.058 | 1.78	0.046 | 1.66	0.042 | 1.32
Seq. 4	0.051 | 1.78	0.045 | 1.49	0.041 | 1.49
Seq. 5	0.055 | 2.46	0.039 | 1.72	0.038 | 1.20
Average	0.053 | 1.89	0.043 | 1.55	**0.040 | 1.32**

The results of real-site experiments. The data in the table are positioning error (m) and heading error (°), separated by vertical symbol.

TABLE IV
COMPARISON WITH RELATED WORKS

Related works	Position	Attitude	Method
UWB-IMU [11]	0.16	-	EKF
UWB-IMU [13]	0.087	-	UKF
UWB-VIO [22]	0.076	-	Optimization
UWB-IMU (ours)	**0.040**	**1.32**	Optimization

Positioning Error (m) and heading Error (°) comparison with related works. The "-" indicates that it is not discussed in the work.

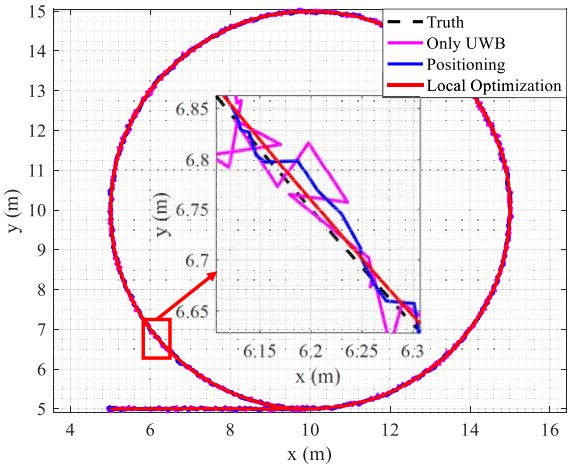

Fig. 6. The simulation experimental trajectories when UWB tags distribution distance is 0.6m.

right triangle. The UWB ranging accuracy is 10 cm. The whole simulation trajectory is show in Fig. 6: firstly, it is stationary for 2s; secondly, it accelerates in a straight line with an acceleration of 1 m/s^2 for 1 s; then it moves forward in a straight line at a constant speed for 4.5 s; finally, it makes a circular motion with a radius of 5 m and a speed of 1 m/s.

1) Influence of UWB Tags Distribution Distance: In order to analyze the influence of different UWB tags distribution distance on system performance, the distance between UWB tags is set as 0.1-1.0 m (increase by 0.1 m each time), and other parameters remain unchanged. The experimental parameters and corresponding results are shown in Fig. 7.

It can be seen that compared with Only UWB, the fusion method has greatly improved the positioning and heading accuracy. With the increase of the distribution distance of UWB tags, the attitude errors of all algorithms are gradually decreasing, and the positioning errors remain unchanged.

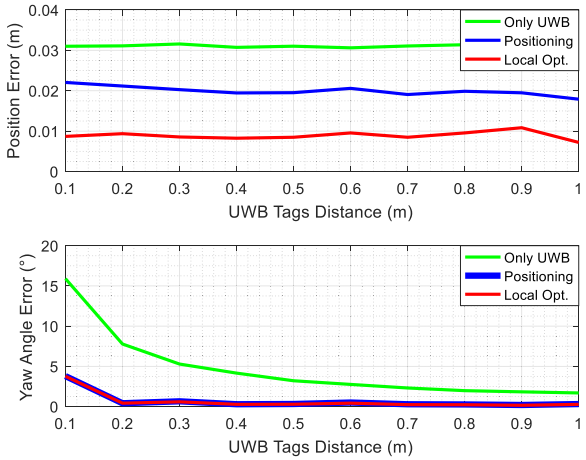

Fig. 7. The influence of UWB tags distribution distance on the system positioning and heading performance.

TABLE V
TIME CONSUMPTION (S) OF DIFFERENT LEVEL ALGORITHMS

Algorithms	Only UWB	Positioning	Local Opt.
Time	0.0006	0.0025	0.0225

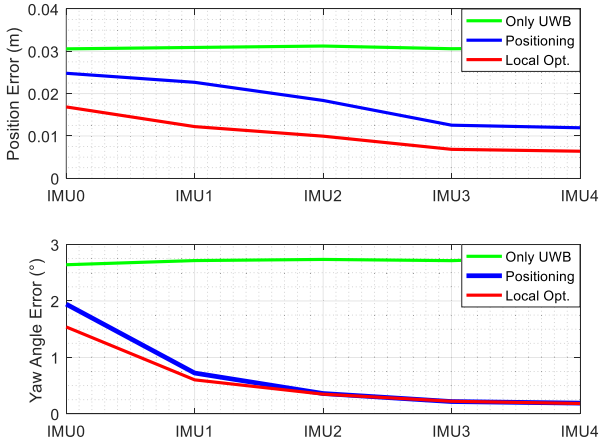

Fig. 8. The influence of IMU Noise Parameters on the system positioning and heading performance.

When the UWB tags distribution distance reaches 0.5 m, the attitude error decreases slowly, and the accuracy of the system can already meet the requirements of conventional applications.

Furthermore, as can be seen from Fig. 6, the Positioning trajectory is smoother than Only UWB trajectory, and the Local Opt. trajectory is the smoothest and closest to the Truth, which is in line with our expectations.

2) Influence of IMU Noise Parameters: This simulation experiment analyzes the influence of different IMU noise parameters on the system performance. The UWB tags distribution distance is set to 0.6 m. The parameters and the corresponding performance of different IMUs (IMU0-IMU4) are shown in Table I and Fig. 8.

The experimental results show that IMU performance has a greater impact on heading accuracy, which can be improved by nearly ten times. For IMU0, due to the noise is too large, there is almost no constraint effect; The performance of IMU3 has reached the extreme, and the smaller IMU noise (IMU4) can hardly continue to improve the accuracy; For the IMU with

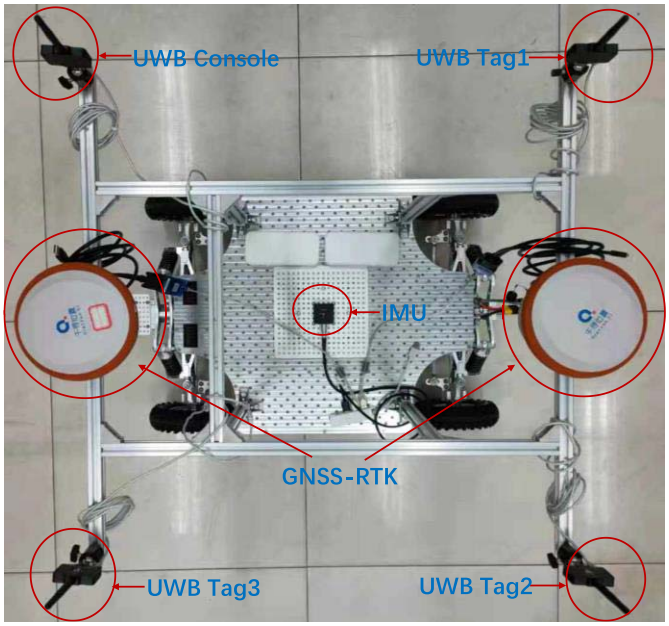

Fig. 9. The UGV platform of our system.

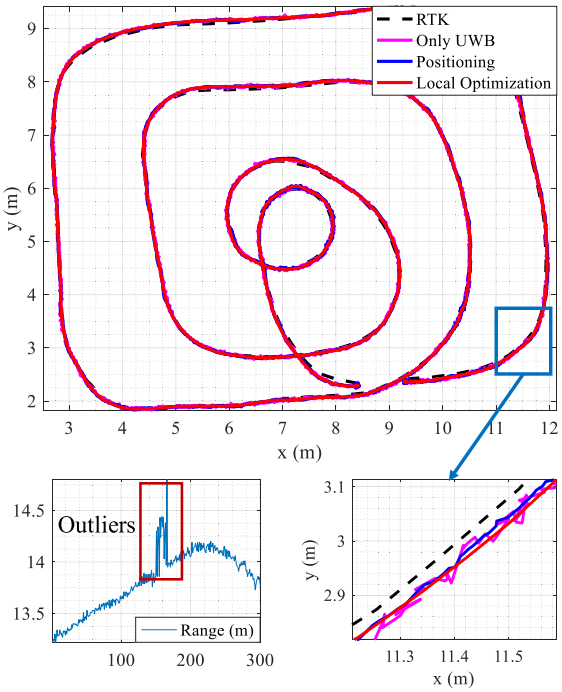

Fig. 10. Experimental results of Seq. 1. The upper figure shows the overall trajectory; The lower right figure shows the partial trajectory, and the lower left figure shows the corresponding ranging measurement between UWB anchor 2 and tag 1.

general performance (between IMU2 and IMU3), the Local Opt. accuracy reaches about 1 cm, which can meet various applications with higher accuracy requirements.

3) Relative Rotation Optimization Verification: In order to verify the ability of our system to optimize the relative rotation, we designed simulation experiments with different rotation angles (0-90°). IMU noise parameters is set to be the same as IMU2 in the previous section, and the UWB tags distribution distance is 0.6 m. The experimental results under different relative rotation are shown in Table II.

The experimental results show that the average attitude error is 2.3°, which can meet the requirement of fusion. Moreover, the relative rotation error after optimization will not change with the change of relative rotation, that is to say, it has good stability and consistency. With this method, the user can avoid some IMU installation problems in practical application.

In short, these simulation experiments prove that our fusion method can not only obtain accurate position and attitude, but also solve the installation problem of IMU, which further expands its application possibilities. Moreover, 3 UWB tags with a 0.5-meter distribution distance and 1 IMU with general performance are sufficient to give full play to the performance of the system, which provides design references for practical applications.

B. Real-Site Experiment

Finally, we test the performance of our system through real-site experiments. The UWB modules we use are LinkTrack P series of NoopLoop, with output frequency of 50 Hz and the nominal ranging accuracy of 10 cm. The IMU module is CHAOHE Electronic consumer grade 6-DOF IMU CH110, with output frequency of 200 Hz. The UWB tags distribution distance is about 0.6m, and the UWB anchors form a rectangle of about 14 m × 11 m. Moreover, 2 GNSS RTK modules (Qianxun SI SE) are used to calculate the position and attitude reference values of Body, and also to calibrate the position of UWB anchors. The accuracy of RTK is about 2 cm. The equipment used in the experiment is shown in Fig. 9.

From the trajectory in Fig. 10, we can see that the result of our algorithm matches the ground truth well, and even if there is a large UWB ranging outlier, it will not affect our result thanks to our outlier elimination algorithm. The results in Table III show that the positioning and heading error of our algorithm can always converge to about 4.0cm and 1.3° respectively, which have approached the accuracy that can be achieved by the RTK used to calibrate the true value. Although system errors, such as installation and calibration, make the positioning accuracy numerically lower than that in simulation experiment, the advantages and effectiveness of Local Opt. can still be clearly seen form the smaller average positioning error, and the trajectory that is closer to the reference value and has less jitter.

Note that in every experiment, we did not calibrate the rotation parameters of the IMU in advance, and IMU data was fused using the results of automatic calibration. Judging from the positioning results, the automatic calibration capability meets the requirements of our algorithm.

The comparison with the latest related works is shown in Table IV. As far as we know, the performance of UWB and IMU modules used in all systems (including ours) in the table are comparable, and our experimental site is the largest. It can be seen that the positioning accuracy of our system is the highest. Moreover, we give a reliable and accurate attitude result that is ignored by most systems, which is also one of the advantages of our system.

C. Running Time Consumption

The algorithm runs on the CPU of low voltage Intel i7-8565U@1.8GHz, the computer system is Ubuntu 16.04, and the project is based on ROS and C++. The corresponding time consumption of different levels of optimization is shown in Table V.

It can be seen that Only UWB can reach thousands of Hertz, and the Positioning can reach hundreds of Hertz, which is enough to meet the needs of real-time positioning. According to our real-time positioning strategy, although the real-time performance of Local Opt. is slightly weak, it does not affect the actual application.

VI. Conclusion

In this paper, a framework based on graph model is proposed to fuse multiple UWBs and IMU for robot state estimation. Through nonlinear optimization and selecting RefFrame as IMU constraint reference, our system supports accurate positioning and heading at the same time, which further expands its application possibility. An optimization method of relative rotation and initial state in motion is designed, which solves the problems of IMU installation direction not easy to measure and dynamic initialization in practical application. The simulation experiment shows the stability and effectiveness of this method. Besides, the influence of IMU property and UWB tags distribution on system performance is analyzed through simulation experiments, which provides design reference and promotes the process of practicality. In addition, our system can be easily extended to the situation of multiple cells and more tags positioning, just need to add more constraints to the graph optimization model.

There are still some areas to be improved. One direction of future work is to calibrate the coordinates of UWB anchors automatically with optimization method. Another point is to extend the application scenarios of this method, such as fusing SLAM to obtain accurate 6DOF state estimation, and to improve the accuracy and function of the system.

References

[1] T. Zhang, "UGV developments in 2020–2030 in terms of technologies," *Digit. Infantry Battlef. Solut. Introd. Gr. Robot.*, pp. 66–78, 2016.

[2] F. Zafari, A. Gkelias, and K. K. Leung, "A survey of indoor localization systems and technologies," *IEEE Commun. Surveys Tuts.*, vol. 21, no. 3, pp. 2568–2599, 3rd Quart., 2017.

[3] G. Shi and Y. Ming, "Survey of indoor positioning systems based on ultra-wideband (UWB) technology," in *Proc. Int. Conf. Wireless Commun., Netw. Appl.*, vol. 348, 2016, pp. 1269–1278.

[4] W. Shule, C. M. Almansa, J. P. Queralta, Z. Zou, and T. Westerlund, "UWB-based localization for multi-UAV systems and collaborative heterogeneous multi-robot systems: A survey," *Proc. Comput. Sci.*, vol. 175, pp. 357–364, Jan. 2020.

[5] J. A. Corrales, F. A. Candelas, and F. Torres, "Hybrid tracking of human operators using IMU/UWB data fusion by a Kalman filter," in *Proc. 3rd Int. Conf. Human Robot Interact. (HRI)*, 2008, pp. 193–200.

[6] A. Benini, A. Mancini, and S. Longhi, "An IMU/UWB/vision-based extended Kalman filter for mini-UAV localization in indoor environment using 802.15.4a wireless sensor network," *J. Intell. Robot. Syst.*, vol. 70, pp. 461–476, May 2013.

[7] Z. Li, G. Chang, J. Gao, J. Wang, and A. Hernandez, "GPS/UWB/MEMS-IMU tightly coupled navigation with improved robust Kalman filter," *Adv. Space Res.*, vol. 58, pp. 2424–2434, Dec. 2016.

[8] Q. Fan, B. Sun, Y. Sun, and X. Zhuang, "Performance enhancement of MEMS-based INS/UWB integration for indoor navigation applications," *IEEE Sensors J.*, vol. 17, no. 10, pp. 3116–3130, May 2017.

[9] Q. Tian, K. I.-K. Wang, and Z. Salcic, "An INS and UWB fusion approach with adaptive ranging error mitigation for pedestrian tracking," *IEEE Sensors J.*, vol. 20, no. 8, pp. 4372–4381, Apr. 2020.

[10] L. Yao, Y.-W.-A. Wu, L. Yao, and Z. Z. Liao, "An integrated IMU and UWB sensor based indoor positioning system," in *Proc. Int. Conf. Indoor Positioning Indoor Navigat. (IPIN)*, Sep. 2017, pp. 1–8.

[11] J. Li, Y. Bi, K. Li, K. Wang, F. Lin, and B. M. Chen, "Accurate 3D localization for MAV swarms by UWB and IMU fusion," in *Proc. IEEE 14th Int. Conf. Control Autom. (ICCA)*, Jun. 2018, pp. 100–105.

[12] M. W. Mueller, M. Hamer, and R. D'Andrea, "Fusing ultra-wideband range measurements with accelerometers and rate gyroscopes for quadrocopter state estimation," in *Proc. IEEE Int. Conf. Robot. Autom. (ICRA)*, May 2015, pp. 1730–1736.

[13] D. Feng, C. Wang, C. He, Y. Zhuang, and X.-G. Xia, "Kalman-filter-based integration of IMU and UWB for high-accuracy indoor positioning and navigation," *IEEE Internet Things J.*, vol. 7, no. 4, pp. 3133–3146, Apr. 2020.

[14] D. Fox, J. Hightower, L. Liao, D. Schulz, and G. Borriello, "Bayesian filtering for location estimation," *IEEE Pervasive Comput.*, vol. 2, no. 3, pp. 24–33, Jul./Sep. 2003.

[15] H. Strasdat, J. M. M. Montiel, and A. J. Davison, "Visual SLAM: Why filter?" *Image Vis. Comput.*, vol. 30, no. 2, pp. 65–77, 2012.

[16] R. Mur-Artal and J. D. Tardos, "ORB-SLAM2: An open-source SLAM system for monocular, stereo, and RGB-D cameras," *IEEE Trans. Robot.*, vol. 33, no. 5, pp. 1255–1262, Oct. 2017.

[17] T. Shan, B. Englot, D. Meyers, W. Wang, C. Ratti, and D. Rus, "LIO-SAM: Tightly-coupled lidar inertial odometry via smoothing and mapping," in *Proc. IEEE/RSJ Int. Conf. Intell. Robots Syst. (IROS)*, Oct. 2020, pp. 5135–5142.

[18] M. Kok, J. D. Hol, and T. B. Schön, "Indoor positioning using ultrawideband and inertial measurements," *IEEE Trans. Veh. Technol.*, vol. 64, no. 4, pp. 1293–1303, Apr. 2015.

[19] A. Perttula, H. Leppäkoski, M. Kirkko-Jaakkola, P. Davidson, J. Collin, and J. Takala, "Distributed indoor positioning system with inertial measurements and map matching," *IEEE Trans. Instrum. Meas.*, vol. 63, no. 11, pp. 2682–2695, Nov. 2014.

[20] C. Hung-Yuan, C.-C. Hou, and Y.-S. Chen, "Indoor intelligent mobile robot localization using fuzzy compensation and Kalman filter to fuse the data of gyroscope and magnetometer," *IEEE Trans. Ind. Electron.*, vol. 62, no. 10, pp. 6436–6447, Oct. 2015.

[21] W. Lv, Y. Kang, and J. Qin, "Indoor localization for skid-steering mobile robot by fusing encoder, gyroscope, and magnetometer," *IEEE Trans. Syst., Man, Cybern., Syst.*, vol. 49, no. 6, pp. 1241–1253, Jun. 2019.

[22] C. Wang, H. Zhang, T.-M. Nguyen, and L. Xie, "Ultra-wideband aided fast localization and mapping system," in *Proc. IEEE/RSJ Int. Conf. Intell. Robots Syst. (IROS)*, Sep. 2017, pp. 1602–1609.

[23] T. H. Nguyen, T.-M. Nguyen, and L. Xie, "Tightly-coupled single-anchor ultra-wideband-aided monocular visual odometry system," in *Proc. IEEE Int. Conf. Robot. Autom. (ICRA)*, May 2020, pp. 665–671.

[24] R. Kummerle, G. Grisetti, H. Strasdat, K. Konolige, and W. Burgard, "G2o: A general framework for graph optimization," in *Proc. IEEE Int. Conf. Robot. Autom.*, May 2011, pp. 3607–3613.

[25] C. Forster, L. Carlone, F. Dellaert, and D. Scaramuzza, "IMU preintegration on manifold for efficient visual-inertial maximum-a-posteriori estimation," *Robot. Sci. Syst.*, vol. 11, 2015.

Shuaikang Zheng received the B.Eng. degree in communication engineering from Shandong University, Shandong, China, in 2018. He is currently pursuing the Ph.D. degree in microelectronics with the State Key Laboratory of Transducer Technology, Aerospace Information Research Institute, Chinese Academy of Sciences, Beijing. His research interests include computer vision and multi-sensor information fusion.

Zhitian Li received the B.Eng. and M.Sc. degrees in electronic science and technology from the School of Optoelectronics, Beijing Institute of Technology, in 2015 and 2018, respectively. Since 2018, he has been an Assistant Research Fellow with the Aerospace Information Research Institute, Chinese Academy of Sciences, Beijing, China. His research interests include sensor fusion technologies, such as optical accelerometer and new generation of PNT systems.

Yunfei Liu received the B.Eng. degree in automation from the University of Science and Technology Beijing, China, in 2017. He is currently pursuing the Ph.D. degree in microelectronics with the State Key Laboratory of Transducer Technology, Aerospace Information Research Institute, Chinese Academy of Sciences, Beijing. His research interests include computer vision, localization of autonomous driving, multi-sensor fusion, and calibration.

Haifeng Zhang received the B.Eng. degree in measurement and control technology and instrument from Zhengzhou University, Henan, China, in 2019. He is currently pursuing the Ph.D. degree in microelectronics with the State Key Laboratory of Transducer Technology, Aerospace Information Research Institute, Chinese Academy of Sciences, Beijing. His research interests include computer vision and SLAM.

Xudong Zou (Member, IEEE) received the B.Sc. degree in microelectronics from Peking University, China, in 2009, and the Ph.D. degree in mechanics, materials, and design from the University of Cambridge, U.K., in 2013. He was with the Nanoscience Center, Department of Engineering, University of Cambridge, as a Research Associate, and the Churchill College, as a Postdoctoral By-Fellow. He is currently a Professor with the State Key Laboratory of Transducer Technology, Institute of Electronics, Chinese Academy of Sciences, and the School of Electronics, Electrical and Communication Engineering, University of Chinese Academy of Sciences. His main research interests include the area of integrated micro and nano-electromechanical systems, with a focus on resonators and inertial sensors, including the design and optimization of high-resolution MEMS resonant inertial sensors, studying the nonlinear effects on the noise processes in MEMS oscillators, and the coupled MEMS resonators in sensing applications. He also works on the sensor fusion technologies, such as SLAM and VIO using MEMS sensors for autonomous navigation.